RESEARCH ARTICLE

WILEY

Functional and structural network changes related with cognition in semantic dementia longitudinally

Lin Huang[1] ⓘ | Liang Cui[1] | Keliang Chen[2] | Zaizhu Han[3] | Qihao Guo[1] ⓘ

[1]Department of Gerontology, Shanghai Sixth People's Hospital Affiliated to Shanghai Jiao Tong University School of Medicine, Shanghai, China

[2]Department of Neurology, Huashan Hospital, Fudan University, Shanghai, China

[3]State Key Laboratory of Cognitive Neuroscience and Learning and IDG/McGovern Institute for Brain Research, Beijing Normal University, Beijing, China

Correspondence
Qihao Guo, Department of Gerontology, Shanghai Sixth People's Hospital Affiliated to Shanghai Jiao Tong University School of Medicine, Shanghai 200233, China.
Email: qhguo@sjtu.edu.cn

Abstract

Longitudinal changes in the white matter/functional brain networks of semantic dementia (SD), as well as their relations with cognition remain unclear. Using a graph-theoretic method, we examined the neuroimaging (T1, diffusion tensor imaging, functional MRI) network properties and cognitive performance in processing semantic knowledge of general and six modalities (i.e., object form, color, motion, sound, manipulation and function) from 31 patients (at two time points with an interval of 2 years) and 20 controls (only at baseline). Partial correlation analyses were carried out to explore the relationships between the network changes and the declines of semantic performance. SD exhibited aberrant general and modality-specific semantic impairment, and gradually worsened over time. Overall, the brain networks showed a decreased global and local efficiency in the functional network organization but a preserved structural network organization with a 2-year follow-up. With disease progression, both structural and functional alterations were found to be extended to the temporal and frontal lobes. The regional topological alteration in the left inferior temporal gyrus (ITG.L) was significantly correlated with general semantic processing. Meanwhile, the right superior temporal gyrus and right supplementary motor area were identified to be associated with color and motor-related semantic attributes. SD manifested disrupted structural and functional network pattern longitudinally. We proposed a hub region (i.e., ITG.L) of semantic network and distributed modality-specific semantic-related regions. These findings support the hub-and-spoke semantic theory and provide targets for future therapy.

KEYWORDS
diffusion tensor imaging, functional neuroimaging, magnetic resonance imaging, semantic dementia, temporal lobes

1 | BACKGROUND

Semantic dementia (SD) is a clinical variant of primary progressive aphasia, characterized by a core symptom of selective and progressive deterioration of semantic knowledge and asymmetrical atrophy/

Lin Huang and Liang Cui contributed equally to this work.

hypometabolism in the anterior temporal lobe (ATL) (Gorno-Tempini et al., 2011). Patients with SD present a distinctive and consistent neuropsychological deficits in semantic knowledge and thus is an ideal lesion model to uncover the organizational principle and neuroanatomic basis of the semantic system (Hodges & Patterson, 2007).

The concept of semantic memory/knowledge was first proposed by Tulving in 1972, which refers to the explicit knowledge about the world (Tulving, 1972). Understanding the representation of semantic knowledge in human brain has long been a topic of great interest in neuroscience. To date, convergent findings tend to support the hub-and-spoke semantic representation theory (Lambon Ralph, 2014; Patterson et al., 2007). According to this theoretical model, the semantic knowledge of how objects look, sound, move and so on is a widely distributed neural network. In addition to these modality-specific regions and connections, the various sensorimotor attributes connect to and communicate through a shared amodal 'hub' to form transmodal/multi-modal general semantic concept. Thus, damage to the semantic hub was expected to lead to deficits in a range of general semantic processing tasks (e.g., oral picture naming, picture association matching), whereas damage to the modality-specific brain areas would cause impairment in the corresponding modality processing assessment (Patterson et al., 2007).

Neuroanatomical facts have supported the view that the semantic hub lies within the ATL, but the precise location varied from the temporal pole, fusiform gyrus, superior temporal gyrus, middle temporal gyrus to the inferior temporal gyrus (ITG) across different studies (Ding et al., 2020; Lambon Ralph, 2014; Patterson et al., 2007). Given that the semantic network is a highly interactive system and the role of altered structural and functional network should be considered. Graph analyses have recently been applied to the brain networks to elucidate the SD-associated topological changes (Nigro, Filardi, et al., 2022). Results from functional MRI studies reported reduced functional connectivity in global/frontolimbic network integration and demonstrated elevated local connectivity within the prefrontal cortex in SD, but evidence regarding the topological properties of white matter network is still lacking (Dev et al., 2021; Pengo et al., 2022). Nevertheless, fewer studies have directly compared the functional and structural network changes in SD. Although the co-localization of structural and functional abnormalities/hypometabolism in SD have been reported in some studies (Acosta-Cabronero et al., 2011; Agosta et al., 2014; Chen et al., 2019), the inconsistencies must also be noted.

This study was intended to unravel the differential structural and functional network topological changes in patients with SD as well as their cognitive performance with disease progression. We adopted a graph-theoretic method and a multimodal imaging approach, that is, grey matter structural (T1), diffusion tensor imaging (DTI) and resting state functional MRI (rs-fMRI), to construct the whole-brain white matter structural and functional networks based on the automated anatomical labeling (AAL) (Tzourio-Mazoyer et al., 2002) atlas in 31 patients at two time points with an interval of 2 years and 20 healthy controls at baseline. We investigated the relationship between brain topological properties and general/modality-specific semantic performance. In this research, we aimed to uncover (i) how would semantic performance progressed in SD as well as their respective structural and functional network patterns over time; (ii) which subregion of ATL or other area would be specifically the hub of semantic network; and (iii) the anatomical underpinnings of modality-specific semantic knowledge in patients with SD.

2 | METHODS

2.1 | Participants

A total of 51 individuals participated in this study, including 31 patients with SD and 20 healthy controls. All were right-handed, native Chinese speakers, had normal or corrected-to-normal hearing and vision, and no history of stroke, head trauma, substance abuse, psychiatric or other neurological diseases. This study was approved by the ethics committees of the Huashan Hospital (Approval number: 2009-195) and the Shanghai Sixth People's Hospital (Approval number: 2022-ky-116). All participants or their person responsible provided written informed consent.

Thirty-one patients with SD that presented to the memory clinic of Huashan Hospital in Shanghai, China, from 2011 to 2018, were recruited with 2-year follow-up (interval months: 24.65 ± 1.66). Meanwhile, 20 healthy controls were recruited from the community through advertising at baseline. Diagnosis was reached by consensus according to the current diagnostic criteria (Gorno-Tempini et al., 2011) following a comprehensive clinical assessment including: medical history, neuropsychological assessment, brain MRI and ^{18}F-FDG PET (Lu et al., 2021). Chinese version of the Mini-Mental State Examination (MMSE) (Katzman et al., 1988) was used to measure the general cognitive function.

2.2 | Neuropsychological data collection and preprocessing

Six general and six modality-specific semantic tasks were designed to evaluate the semantic behavior of all the participants. General semantic tasks measured the multi-modal semantic knowledge. The modality-specific semantic tasks examined semantic knowledge on six specific sensorimotor aspects, that is, form, color, motion, sound, manipulation and function. Three nonsemantic control tasks involving no or minimal semantic processing were also assessed. These tasks were already used in our recent study (Chen et al., 2020) (see Supplementary Material for details).

We used a principal component analysis (PCA) to extract the generalized semantic performance, detailed in Supplementary Results 2. Component 1 had a highest loading weight on the six general semantic tasks and low loading weight on the three nonsemantic control tasks, thus the scores derived from this component were considered to represent general semantic ability (see Supplementary Material Table S1).

2.3 | Brain MRI acquisition

All individuals underwent a whole-brain MRI with a 3T Siemens scanner at Huashan Hospital, including an anatomical T1 scan, a diffusion weighted scan, and a resting-state functional scan. All the MRI data was obtained with the same scanner including the follow-up (see Supplementary Material for details).

2.4 | Imaging data preprocessing

T1-weighted images were preprocessed using the computational anatomy toolbox (CAT) in Statistical Parametric Mapping (SPM12) software (https://www.fil.ion.ucl.ac.uk/spm/software/spm12/). Diffusion-weighted images were preprocessed using a pipeline for analyzing brain diffusion images (PANDA, 2016.1.3.1, https://www.nitrc.org/projects/panda). Rs-fMRI data were preprocessed using the graph theoretical network analysis toolbox (GRETNA, v2.0.0, https://www.nitrc.org/projects/gretna/) (see Supplementary Material for details).

2.5 | Constructing networks

Two basic elements, nodes and edge, are required for the network construction. For comparison across white matter and functional networks, a prior atlas of AAL (Tzourio-Mazoyer et al., 2002) was used to divide the whole brain into 90 regions, where each region represented a network node. These network construction methods for both DTI and rs-fMRI data are based on approaches previously reported (Chen et al., 2015; Wang et al., 2015) and detailed below.

We used PANDA to construct the whole-brain white matter network. Deterministic tractography was performed in the native space using FACT (Mori et al., 1999). Specifically, we defined the number of fiber tracts (FN) between two nodes as the weight of the network edges. Thus, for each participant we constructed the FN-weighted white matter network represented by a 90×90 matrix. Finally, to determine whether a node pair was anatomically connected, we used a group-level threshold of 0.8 to ensure that at least 80% of subjects had a connection between two brain regions.

To construct functional network, a mean time series was extracted from each parcellated region (node), and linear Pearson correlation coefficients were then calculated to estimate pairwise functional connectivity as the measurement of network edges. Then, a 90×90 correlation network matrix was yielded for each individual. The absolute values (composed of both positive correlations and negative correlations) were calculated and a binary network was obtained for each participant for further analysis.

2.6 | Network analysis

We calculated several widely used global and nodal network graph metrics to characterize the topological organization of both white matter and functional networks. Global graph measures include local and global efficiency, which reflect how well the information propagates throughout the network (Rubinov & Sporns, 2010). We also calculated the clustering coefficient, characteristic path length, small-worldness, and assortativity to additionally evaluate the network efficiency for information processing. For regional nodal characteristics, nodal degree centrality (the number of connections linked directly to a node) and nodal efficiency (how efficient a node communicates with the others) were estimated to reflect the importance of the node in the network (Wang et al., 2011). Note that for the analysis of functional network, we used a sparsity threshold of the resultant network ranging from 0.05 to 0.4 with an interval of 0.01 and calculated the area under the curve (AUC) for each network measure to provide a scalar that did not depend on a specific threshold selection.

Network analysis was applied using GRETNA and visualized using BrainNet Viewer (www.nitrc.org/projects/bnv/).

2.7 | Statistical analysis

Statistical analyses were performed using SPSS Statistics 21.0 (IBM Corp., Armonk, NY) and GRETNA 2.0.0 software. The significance level was set at $p < .05$ (two-tailed) across all comparisons. We compared demographic data between groups by means of independent two-sample t-tests at baseline and paired t-test at follow-up. Chi-square test was performed to assess sex difference. For comparison of behavioral performance and network metrics between patients and healthy controls, an analysis of covariance (ANCOVA) was used to evaluate between-group differences (adjusted age, sex, and education). Longitudinal data in SD group between two time points was analyzed using a repeated measure of ANCOVA to minimize the potential bias of age, sex, or education. We assumed minimal change in the control group over time, and therefore did not include them in the longitudinal analyses. To evaluate the statistical differences in multiple nodal metrics, we applied the FDR method to correct the multiple comparisons. Partial correlation analyses were used to assess the relationships between graph metrics and behavioral performance, controlling for age, sex, and education. FDR method was also used to correct for multiple comparisons of partial correlation analyses.

3 | RESULTS

3.1 | Demographic and cognitive performance

See Table 1. No differences in age, sex, or education were found between SD and control groups. Notably, only a portion (23/31) of the patients had available fMRI data. Participants' raw scores on the semantic assessments are shown in Table 2. After controlling for the effects of age, sex, and education, the SD group exhibited profound deficits in the general semantic tasks and almost all modality-specific

TABLE 1 Demographics and neuropsychological tests.

Index	Healthy controls (baseline), n = 20	Semantic dementia (baseline), n = 31	Semantic dementia (follow-up), n = 31	Baseline comparison			Follow-up comparison		
				T/χ^2	Df	p	T	Df	p
Age (years)	60.50 ± 3.85	63.13 ± 6.22	64.9 ± 6.28	−1.66	49	.104	NA	NA	NA
Sex (Male:Female)	8:12	14:17	14:17	0.132	1	.716	NA	NA	NA
Education (years)	10.45 ± 2.82	12.13 ± 3.44	12.13 ± 3.44	−1.79	49	.080	NA	NA	NA
Disease duration (years)	-	3.58 ± 0.94	5.63 ± 0.92	NA	NA	NA	NA	NA	NA
DTI/fMRI	20/20	31/23	31/23	NA	NA	NA	NA	NA	NA
General mental status									
MMSE (max = 30)	28.10 ± 1.373	22.48 ± 3.723	17.10 ± 4.61	6.45	49	<.001*	6.62	30	<.001*
Language									
BNT (max = 30)	22.10 ± 3.28	6.81 ± 3.93	3.35 ± 3.55	14.46	49	<.001*	4.18	30	<.001*
Memory									
CFT delayed recall (max = 36)	16.55 ± 6.57	11.16 ± 5.86	7.48 ± 5.98	3.06	49	.004*	3.26	30	.003*
Visuo-spatial function									
CFT copy (max = 36)	34.25 ± 2.02	32.48 ± 3.58	31.39 ± 5.58	2.01	49	.05	1.74	30	.092
Executive function									
TMT-B, seconds	147.10 ± 43.80	176.52 ± 70.16	201.03 ± 82.16	−1.67	49	.101	−1.56	30	.130
Calculation (max = 7)	6.50 ± 0.69	6.61 ± 0.67	6.52 ± 0.51	−0.58	49	.563	0.90	30	.374

Note: Values are expressed as mean ± standard deviation.
Abbreviations: BNT, Boston naming test; CFT, complex figure test; DTI/fMRI, numbers of individuals with MRI scans; df, degree of freedom; MMSE, mini-mental state examination; NA, not applicable; TMT-B, trail making test-part B.
*p < .05.

semantic tasks compared with healthy controls at baseline. From a longitudinal perspective, patients showed significant decline in both general and modality-specific semantic tasks. No significant decline was observed in nonsemantic control tasks.

3.2 | Cerebral atrophy pattern

Figure 1 illustrates the comparison of the grey matter volume between patients and controls at baseline and follow-up (p < .01, FDR-corrected). Patients demonstrated most severe atrophy in bilateral temporal lobes, insula and ventral frontal lobes at baseline, and extended to more posterior temporal regions, frontal, parietal and occipital areas.

3.3 | Global topological organization of SD

The global and local efficiency of overall functional and white matter networks were depicted in Figure 2. At baseline, no significant difference in the global efficiency was found between patients and controls in both the functional ($F_{[1,38]} = 0.10$, p = .757, patients: 0.180 ± 0.010, controls: 0.182 ± 0.009) and white matter

($F_{[1,46]} = 0.14$, p = .712, patients: 0.231 ± 0.035, controls: 0.244 ± 0.012) network; Likewise, there was no significant difference in the local efficiency of the functional ($F_{[1,38]} = 3.64$, p = .063, patients: 0.255 ± 0.010, controls: 0.255 ± 0.009) and white matter ($F_{[1,46]} = 3.47$, p = .069, patients: 0.365 ± 0.047, controls: 0.391 ± 0.035) network. At 2-year follow-up, patients had a significantly decreased global efficiency ($F_{[1,41]} = 4.57$, p = .038, 0.172 ± 0.013) and lower local efficiency ($F_{[1,41]} = 4.76$, p = .034, 0.247 ± 0.014) in the functional network; while no significant difference was observed in the white matter network (global efficiency: 0.222 ± 0.041, $F_{(1,57)} = 1.32$, p = .256; local efficiency: 0.360 ± 0.065, $F_{(1,57)} = 0.06$, p = .814). Moreover, we observed a decreased small-worldness, and a higher characteristic path length in the global functional network organization with disease progression. Results of other global network measures such as clustering coefficient, characteristic path length, small-worldness, and assortativity were provided in Supplementary Table S2.

3.4 | Regional topological organization of SD

The differences in nodal metrics (degree centrality and nodal efficiency) among each group depicted the alterations in regional

TABLE 2 Baseline performance and annualized decline on the primary behavioral outcome variables.

Neuropsychological assessments	Semantic dementia, n = 31	Annual decline (%), n = 31	Healthy controls, n = 20	Baseline comparison			Follow-up comparison		
				F	Df	p	F	Df	p
General semantic task									
Oral picture naming (max = 140)	47.77 ± 27.47	27.67 ± 15.00	125.65 ± 7.20	125.97	1, 46	<.001***	15.93	1, 55	<.001***
Oral sound naming (max = 36)	8.74 ± 4.41	28.62 ± 35.40	26.95 ± 4.48	173.71	1, 46	<.001***	23.39	1, 55	<.001***
Picture associative matching (max = 70)	52.48 ± 6.90	7.08 ± 5.29	66.45 ± 2.40	62.72	1, 46	<.001***	15.00	1, 55	<.001***
Word associative matching (max = 70)	53.13 ± 8.33	7.21 ± 6.23	67.15 ± 1.46	49.04	1, 46	<.001***	14.69	1, 55	<.001***
Word-picture verification (max = 70)	44.39 ± 15.23	17.76 ± 13.57	67.25 ± 1.94	35.65	1, 46	<.001***	18.70	1, 55	<.001***
Naming to definition (max = 70)	16.87 ± 13.91	27.41 ± 19.15	58.40 ± 5.77	137.76	1, 46	<.001***	12.87	1, 55	<.001***
Modality-specific semantic task									
Verbal task									
Form matching (max = 75)	56.32 ± 8.95	10.11 ± 11.27	70.10 ± 3.26	42.39	1, 46	<.001***	16.27	1, 55	<.001***
Color matching (max = 30)	20.68 ± 3.69	8.25 ± 9.65	28.40 ± 1.31	65.01	1, 46	<.001***	17.50	1, 55	<.001***
Motion matching (max = 30)	19.47 ± 4.22	11.32 ± 14.44	27.70 ± 1.49	57.12	1, 46	<.001***	17.83	1, 55	<.001***
Sound matching (max = 45)	30.37 ± 3.21	7.14 ± 7.27	36.90 ± 3.74	38.81	1, 46	<.001***	18.35	1, 55	<.001***
Manipulation matching (max = 30)	21.10 ± 4.41	8.55 ± 14.27	27.50 ± 1.57	31.54	1, 46	<.001***	14.58	1, 55	<.001***
Function matching (max = 60)	47.93 ± 7.36	11.58 ± 10.44	58.85 ± 1.14	43.71	1, 46	<.001***	22.51	1, 55	<.001***
Nonverbal task									
Form verification (max = 60)	32.03 ± 9.00	7.64 ± 10.02	48.85 ± 4.00	55.69	1, 46	<.001***	3.87	1, 55	.054
Color verification (max = 20)	8.03 ± 3.24	5.45 ± 44.18	14.10 ± 2.02	48.94	1, 46	<.001***	5.50	1, 55	.023*
Motion verification (max = 57)	22.27 ± 8.80	19.70 ± 18.41	32.65 ± 7.39	19.01	1, 46	<.001***	15.44	1, 55	<.001***
Sound verification (max = 42)	15.03 ± 5.75	10.38 ± 17.41	32.95 ± 3.90	124.08	1, 46	<.001***	8.19	1, 55	.006**
Manipulation verification (max = 20)	14.90 ± 1.94	3.36 ± 11.01	15.25 ± 1.80	0.98	1, 46	.328	5.97	1, 55	.018*
Function verification (max = 30)	23.29 ± 2.81	4.29 ± 7.89	27.35 ± 1.70	26.30	1, 46	<.001***	7.71	1, 55	.007**
Nonsemantic control task									
Visual perception (max = 30)	27.84 ± 1.39	0.85 ± 3.13	27.25 ± 1.62	2.61	1, 46	.113	0.77	1, 55	.384
Sound perception (max = 44)	36.26 ± 4.43	2.28 ± 8.75	38.55 ± 4.36	3.38	1, 46	.072	2.13	1, 55	.150
Number proximity matching (max = 3)	2.71 ± 0.59	−4.57 ± 28.00	2.80 ± 0.41	0.62	1, 46	.434	0.01	1, 55	.912

Note: Values are expressed as mean ± standard deviation.

Abbreviation: *df*, degree of freedom.
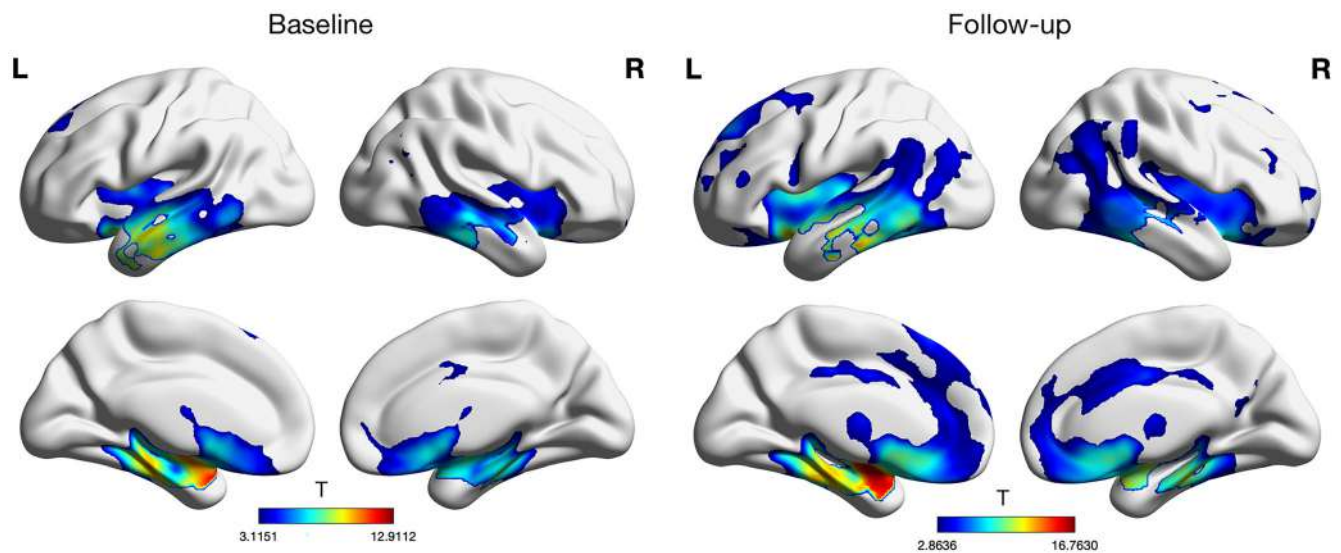
*p < .05; **p < .01; ***p < .001.

FIGURE 1 Brain atrophy map of semantic dementia. The figure shows the areas with significant differences in gray matter volume between semantic dementia and healthy controls at baseline and follow-up ($p < .01$, FDR-corrected).

topography across the functional and structural network (Figure 3, Supplementary Table S3).

At baseline in the white matter network, a number of temporal and frontal/prefrontal regions showed marginal decreases in degree centrality in SD group, including the left inferior temporal gyrus (ITG.L), bilateral olfactory cortex (OLF), opercular part of right inferior frontal gyrus (IFGoperc.R), right gyrus rectus (REC.R), medial orbital part of right superior frontal gyrus (ORBsupmed.R), and right supplementary motor area (SMA.R). Meanwhile, two regions showed changes in nodal efficiency, including decreased ITG.L and increased SMA.R. In the functional network, increased nodal efficiency was obtained in the left middle frontal gyrus (MFG.L).

At follow-up, numerous brain areas showed longitudinal changes in regional topologies, but none survived the correction for multiple comparisons. In the white matter network, the right superior temporal gyrus (STG.R) and paracingulate gyrus (ACG.L) showed significant decreased degree centrality. In the functional network, the right temporal lobe of superior temporal gyrus (TPOsup.R) and bilateral amygdala (AMYG) showed decreased degree centrality. Otherwise, decline in nodal efficiency was observed in the AMYG.L in the functional network.

3.5 | Relations between nodal metrics and semantic performance

To explore the general and modality-specific semantic-related regions, the relations between degree centrality of white matter network and semantic performance were investigated (see Figure 4). The six general semantic tasks (Table 1) examined the general ability of semantic processing with various modalities of input and output, thus the nodal metrics which are significantly correlated to the semantic PCA scores

derived from these tasks could be the hub region linking different aspect of semantic knowledge.

At baseline, only the ITG.L degree centrality of white matter network was identified to be positively correlated with general semantic processing extracted by PCA analysis (see Supplementary Material in detail), after controlling for age, sex, and education ($r = 0.523$, $p = .018$, FDR-corrected).

At follow-up, the differences of degree centrality in white matter network and cognitive performance in patients were calculated before and after, and their correlations were analyzed accordingly, adjusted for age, sex, and education. The decreased STG.R was positively correlated with color verification ($r = 0.444$, $p = .018$, FDR-uncorrected); and decreased SMA.R was positively correlated with manipulation matching ($r = 0.565$, $p = .002$, FDR-corrected) and motion matching ($r = 0.432$, $p = .022$, FDR-uncorrected). Moreover, the declined ITG.L was observed to be positively correlated with function verification ($r = 0.606$, $p = .001$, FDR-corrected), manipulation verification ($r = 0.593$, $p = .001$, FDR-corrected) and motion matching ($r = 0.476$, $p = .01$, FDR-uncorrected).

4 | DISCUSSION

Our study evaluated the topological changes in brain white matter and functional network as well as cognitive performance in 31 SD at two time points with 2-year follow-up. We measured the correlation between regional nodal metrics with patients' semantic performance. Results showed that SD exhibited aberrant general and modality-specific semantic impairment compared to healthy controls, and gradually worsened over time. Overall, the brain networks of SD showed a decreased global and local efficiency in the functional network organization but a preserved structural network organization at follow-up. With disease progression, both structural and functional alterations were found to be extended to the
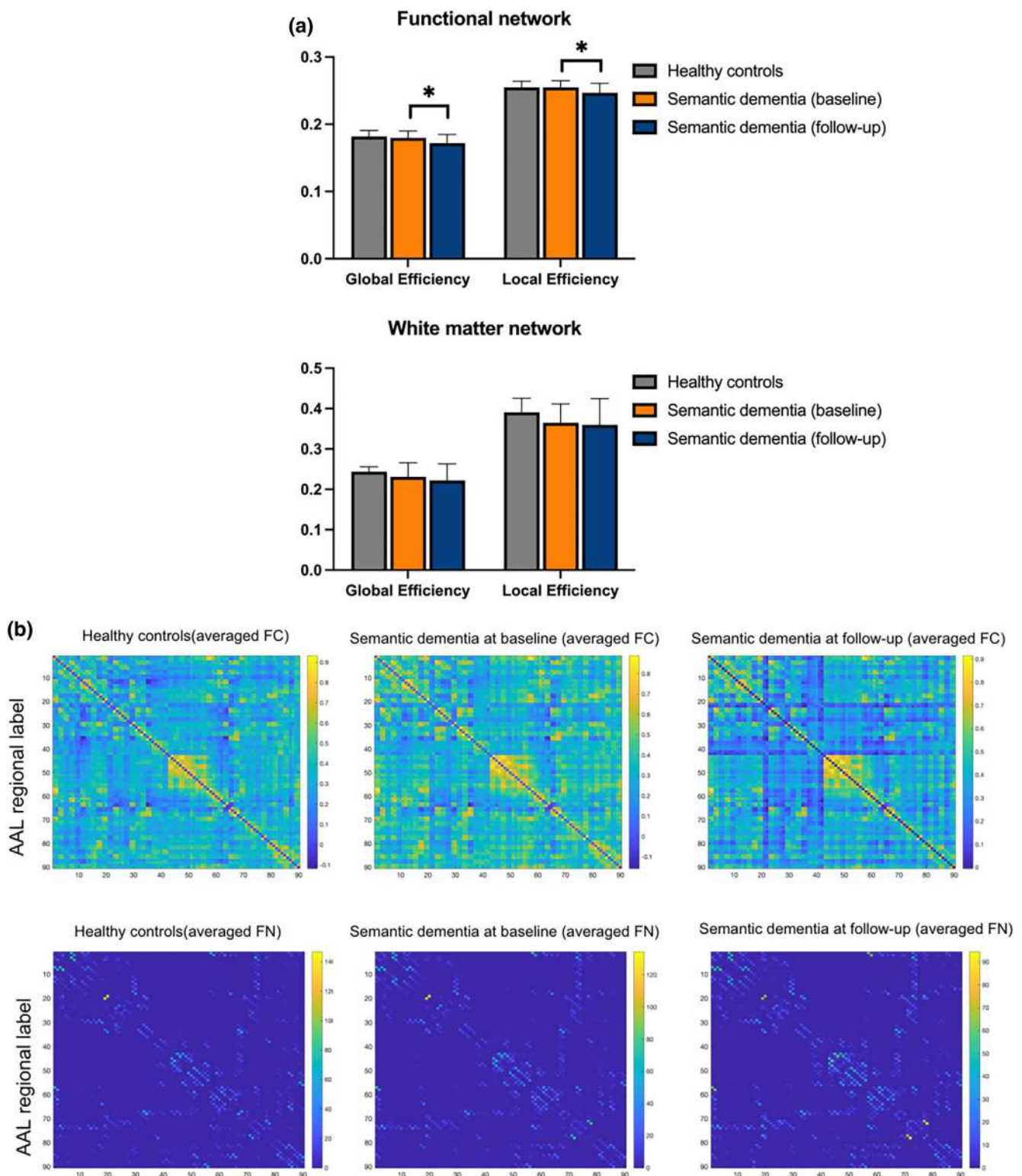
FIGURE 2   Global measures for functional and white matter network. (a) Group differences in global graph properties of functional and structural networks were quantified for semantic dementia and healthy controls at baseline and follow-up, adjusted for age, sex, and education. Error bars represent the standard deviation. (b) Functional and white matter brain network matrices weighted by averaged functional connectivity (FC) and averaged fiber numbers (FN) in patients and controls. Note that these matrices are symmetrical.

temporal and frontal lobes. Finally, we found that the ITG.L was significantly correlated with general semantic processing and suggested to be the hub of semantic network. Moreover, the modality-specific semantic knowledge was located in distributed regions. To our knowledge, this is the first study to report the longitudinal functional and structural network pattern related with semantic performance in a relatively large SD sample size.
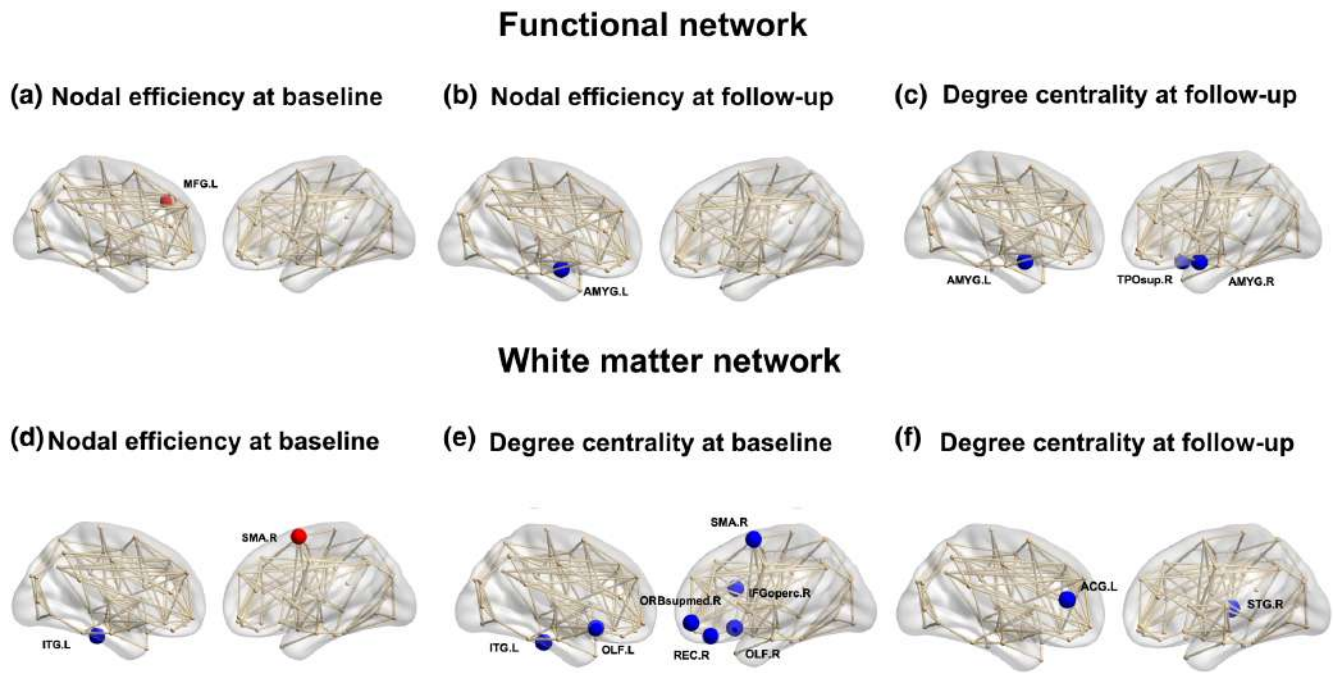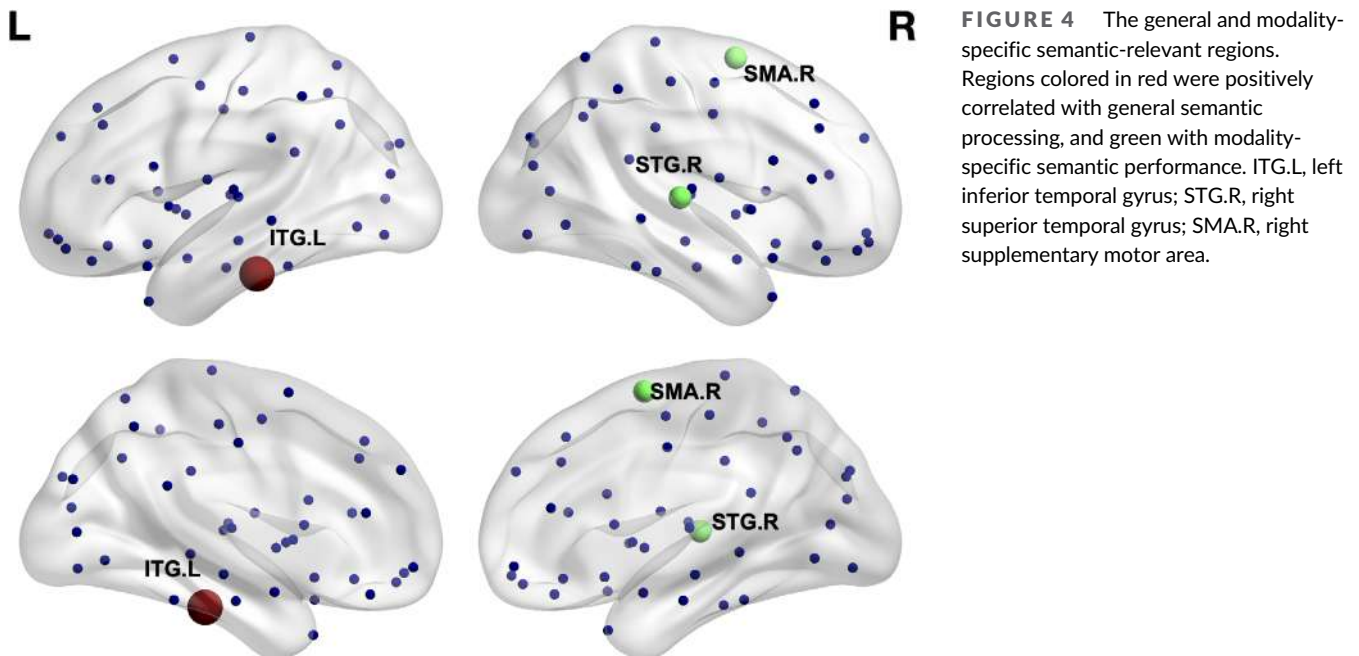
Functional network

(a) Nodal efficiency at baseline

(b) Nodal efficiency at follow-up

(c) Degree centrality at follow-up

White matter network

(d) Nodal efficiency at baseline

(e) Degree centrality at baseline

(f) Degree centrality at follow-up

FIGURE 3 Brain regions demonstrated significant group differences in regional nodal metrics. Regions colored in red showed increased nodal metrics, and blue with decreased nodal metrics in semantic dementia in the functional (a–c) and white matter (d–f) network ($p < .05$). ACG, anterior cingulate and paracingulate gyri; AMYG, amygdala; IFGoperc, inferior frontal gyrus; ITG, inferior temporal gyrus; MFG, middle frontal gyrus; OLF, olfactory cortex; opercular part; ORBsupmed, superior frontal gyrus, medial orbital; REC, gyrus rectus; SMA, supplementary motor area; STG, superior temporal gyrus; TPOsup, temporal pole: superior temporal gyrus.

FIGURE 4 The general and modality-specific semantic-relevant regions. Regions colored in red were positively correlated with general semantic processing, and green with modality-specific semantic performance. ITG.L, left inferior temporal gyrus; STG.R, right superior temporal gyrus; SMA.R, right supplementary motor area.

4.1 | Semantic performance with disease progression

In accordance with our previous study (Chen et al., 2020), patients displayed marked impairments in both general and modality-specific semantic performance, and deteriorated gradually at follow-up. In verbal tasks, the decreases in six different tasks from baseline to year 2 were of similar magnitude, whereas in nonverbal tasks, the patients tended to have a larger decrease in motion verification but not in manipulation/function verification. It indicated that in nonverbal semantic tasks, the impairments of motion and manipulation/function in SD were separated.

4.2 | Disrupted organization of structural and functional networks in SD

At baseline, disrupted structural and functional network changes were demonstrated in SD group. Regional abnormalities in the left temporal and bilateral frontal were identified in the white matter network, whereas changes in the left prefrontal areas were recognized in the functional network. At follow-up, decreased nodal metrics extended to temporal and frontal lobes in both functional and structural networks. These areas, functioned as association, paralimbic and subcortical, were also reported to have decreased or increased functional activation in previous studies (Bejanin et al., 2019; Schwab et al., 2020).

It has been reported that the peak atrophy in SD at baseline was in the TPOsup, extending to the left middle temporal and ITG, fusiform, AMYG, and anterior cingulate cortex; With disease progression, atrophy becomes more distributed to the middle and inferior frontal lobes, posterior temporal gyrus, and inferior parietal areas (Collins et al., 2017; Peet et al., 2021; Planche et al., 2023). Although it has been widely accepted that SD is associated with predominant atrophy of ATL, limited evidence is available regarding both the structural and functional network abnormalities, especially the changes with disease progression. Advanced multi-modal neuroimaging, such as fMRI, DTI and PET, has been essential to uncover the underlying neuropathology and explore preclinical stages, with a greater sensitivity than single structural MRI (Jiskoot et al., 2019; Younes & Miller, 2020). For instance, the utilization of FDG-PET to distinguish different patterns of metabolic abnormalities is also a promising approach to predict progression to SD (Cerami et al., 2017). The FDG-PET allowed the assessment of local and long-range disconnections in neural networks, and was able to identify dysfunctional connectivity patterns in different variants of frontotemporal dementia (FTD), providing complementary results of structural and functional MRI and contributing to a more accurate classification of these patients (Bejanin et al., 2019, 2020; Malpetti et al., 2019). However, although studies have reported extensive changes in both structural and functional connectome in SD, less is known about how these changes are related to the semantic symptoms from a longitudinal perspective. The current available researches are mostly based on cross-sectional data. Only a minority follow-up studies to date have been somewhat limited by small sample size (Bejanin et al., 2020; Binney et al., 2017; Cousins et al., 2018; Kumfor et al., 2016; Staffaroni et al., 2019; Younes et al., 2022), and even none containing both functional and structural network analysis.

In the current study, we used the global and local graph properties to identify specific patterns of functional and structural alterations and investigated the neural correlates of cognitive performance in SD. Graph theory allows describing the brain as a complex network identifying topological properties that reflects global and local information communication, which has been increasingly applied in evaluating the brain connectivity in FTD (Nigro, Filardi, et al., 2022). Recent studies have reported that the abnormalities of SD in brain structure and function were predominantly in the frontal, temporal, and subcortical regions, progressing to posterior areas eventually (Yu

et al., 2021). In this study, patients presented with a similar distribution of abnormal network variation including the temporal and frontal regions. Moreover, we observed a decreased global and local efficiency, a decreased small-worldness, and a higher characteristic path length in the global functional network organization in SD, which could reflect lower integration in the overall brain functional network but a preserved structural network organization with 2-year follow-up. To date, only a few studies adopted graph theory analysis and demonstrated decreased global efficiency in the global functional network organization of SD cross-sectionally (Agosta et al., 2014; Reyes et al., 2018; Tao et al., 2020). Another recent research also observed a reduced small-worldness in the structural brain network in patients with SD (Nigro et al., 2022). At the local level, reduced degree centrality and nodal efficiency were found in the left middle and superior temporal lobes, fusiform, AMYG, entorhinal cortex, hippocampus, and insula (Agosta et al., 2014; Nigro et al., 2022). These studies are partially concordant with our results and further confirmed our findings.

4.3 | The semantic hub and distributed modality-specific semantic knowledge

Only the ITG.L was found positively correlated with general semantic processing. With disease progression, decreased ITG.L degree centrality was associated with decline of multi-modal semantic tasks. These findings indicated that the ITG.L was pivotal in multi-modal semantic processing, and had the potential to be the hub in semantic network. The atrophy of ITG.L has been reported to be associated with semantic tasks (Boeve et al., 2022; Playfoot et al., 2018). However, previous studies did not directly clarify the critical role of ITG.L in combining multimodal knowledge within the semantic network.

Since the ITG.L is also a subregion of ATL, our study supports the notion that the hub of semantic network lies in the ATL. Notably, this result is a bit different from our previously published research indicating the left fusiform gyrus as the hub region (Chen et al., 2020). Anatomically, the ventral surface of ATL is separated by the occipito-temporal sulcus, where the fusiform gyrus is located medially and the ITG is laterally (Lin et al., 2020). Thus in this study, semantic activation was revealed in a more lateral ATL region. The ITG is connected to frontal, parietal and occipital lobes via multiple tracts of connecting pathway (e.g., arcuate fasciculus, inferior longitudinal fasciculus, U-fiber); It is also connected to the superior/middle temporal gyri, entorhinal cortex, and fusiform gyrus via short association fibers within the temporal lobe. The presence of these fiber tracts suggests the function of ITG in semantic processing (Agosta et al., 2010; Lin et al., 2020). One study investigated the semantic activation using fMRI, SD atrophy and transcranial magnetic stimulation (TMS). They obtained activation in the ATL region and was centered on the left fusiform gyrus and the ITG.L (Binney et al., 2010). Another study comparing the functional connectivity changes in behavioral, semantic, and nonfluent variants of FTD has reported a major disconnection of the ITG.L in patients with SD (Reyes et al., 2018). As the fusiform gyrus is far away from the scalp, the ITG.L could be an alternative for

the target brain region of TMS treatment. Therefore, our findings also provide a rationale for therapeutic development in future studies.

Although recent studies have provided convergent evidence for the distributed-plus-hub semantic representation model, there are still ongoing debates about how different aspects of semantic knowledge are distributed across human brain. Some studies hypothesized that semantic attributes were tightly yet separately packed into the posterior temporal, frontal and inferior parietal areas (Reber et al., 2019; Woollams & Patterson, 2018). For example, one study reported three key white matter tracts linking the ATL with module-related cortices, that is, written word forms (fusiform face area), abstract lexical representations (posterior/superior temporal cortices), and face/object representations (visual word form area) (Sundqvist et al., 2020). Our results revealed that the STG.R was associated with color attribute, and the SMA.R was associated with function, motion and manipulation attributes, supporting the notion that different aspects of semantic knowledge are stored in distributed brain areas. Some previous studies offered similar insights. For example, one neuroimaging research demonstrated that performing color perception tasks activated the ventral temporal gyrus (Simmons et al., 2007); and the SMA.R was located in the frontal area, which was also reported to be substantial for the manipulation of the semantic database (Vignando et al., 2020; Wagner et al., 2001).

Limitations should be noted. First, we did not examine the direct relationships between functional/structural connectivity and cognitive performance. As the artefact/noise was higher in fMRI, and not all patients had both modalities performed, the results have to be interpreted with caution. Further studies with complementary techniques such as the metabolic connectivity analysis of FDG-PET scans might have the potential to detect early changes in the functional networks with lower noise level. Second, some nodal metrics did not observe significant results surviving the correction for multiple comparisons. An enlarging of sample size could further verify our findings. Third, this study only included longitudinal data for patients with SD, lacking follow-up results for the control group. Future studies exploring the longitudinal differences between SD and NC groups would provide more evidence supporting our conclusion. Finally, the noncognitive behavioral symptoms rather than language problems in patients with SD, such as disinhibition, irritability, apathy and loss of empathy deserve greater attention. These issues need to be addressed in future research.

ACKNOWLEDGMENTS

CONFLICT OF INTEREST STATEMENT

The authors have no competing interests to declare.

DATA AVAILABILITY STATEMENT

All data and study materials are available from the corresponding author on reasonable request.

ORCID

Lin Huang https://orcid.org/0000-0003-1359-6096
Qihao Guo https://orcid.org/0000-0001-5079-8047

REFERENCES

Acosta-Cabronero, J., Patterson, K., Fryer, T. D., Hodges, J. R., Pengas, G., Williams, G. B., & Nestor, P. J. (2011). Atrophy, hypometabolism and white matter abnormalities in semantic dementia tell a coherent story. *Brain: A Journal of Neurology*, *134*(Pt 7), 2025–2035. https://doi.org/10.1093/brain/awr119

Agosta, F., Galantucci, S., Valsasina, P., Canu, E., Meani, A., Marcone, A., Magnani, G., Falini, A., Comi, G., & Filippi, M. (2014). Disrupted brain connectome in semantic variant of primary progressive aphasia. *Neurobiology of Aging*, *35*(11), 2646–2655. https://doi.org/10.1016/j.neurobiolaging.2014.05.017

Agosta, F., Henry, R. G., Migliaccio, R., Neuhaus, J., Miller, B. L., Dronkers, N. F., Brambati, S. M., Filippi, M., Ogar, J. M., Wilson, S. M., & Gorno-Tempini, M. L. (2010). Language networks in semantic dementia. *Brain: A Journal of Neurology*, *133*(Pt 1), 286–299. https://doi.org/10.1093/brain/awp233

Bejanin, A., La Joie, R., Landeau, B., Belliard, S., de La Sayette, V., Eustache, F., Desgranges, B., & Chételat, G. (2019). Distinct interplay between atrophy and hypometabolism in Alzheimer's versus semantic dementia. *Cerebral Cortex (New York, NY: 1991)*, *29*(5), 1889–1899. https://doi.org/10.1093/cercor/bhy069

Bejanin, A., Tammewar, G., Marx, G., Cobigo, Y., Iaccarino, L., Kornak, J., Staffaroni, A. M., Dickerson, B. C., Boeve, B. F., Knopman, D. S., Gorno-Tempini, M., Miller, B. L., Jagust, W. J., Boxer, A. L., Rosen, H. J., & Rabinovici, G. D. (2020). Longitudinal structural and metabolic changes in frontotemporal dementia. *Neurology*, *95*(2), e140–e154. https://doi.org/10.1212/WNL.0000000000009760

Binney, R. J., Embleton, K. V., Jefferies, E., Parker, G. J. M., & Ralph, M. A. L. (2010). The ventral and inferolateral aspects of the anterior temporal lobe are crucial in semantic memory: Evidence from a novel direct comparison of distortion-corrected fMRI, rTMS, and semantic dementia. *Cerebral Cortex (New York, NY: 1991)*, *20*(11), 2728–2738. https://doi.org/10.1093/cercor/bhq019

Binney, R. J., Pankov, A., Marx, G., He, X., McKenna, F., Staffaroni, A. M., Kornak, J., Attygalle, S., Boxer, A. L., Schuff, N., Gorno-Tempini, M., Weiner, M. W., Kramer, J. H., Miller, B. L., & Rosen, H. J. (2017). Data-driven regions of interest for longitudinal change in three variants of frontotemporal lobar degeneration. *Brain and Behavior*, *7*(4), e00675. https://doi.org/10.1002/brb3.675

Boeve, B. F., Boxer, A. L., Kumfor, F., Pijnenburg, Y., & Rohrer, J. D. (2022). Advances and controversies in frontotemporal dementia: Diagnosis, biomarkers, and therapeutic considerations. *The Lancet: Neurology*, *21*(3), 258–272. https://doi.org/10.1016/S1474-4422(21)00341-0

Cerami, C., Dodich, A., Greco, L., Iannaccone, S., Magnani, G., Marcone, A., Pelagallo, E., Santangelo, R., Cappa, S. F., & Perani, D. (2017). The role of single-subject brain metabolic patterns in the early differential diagnosis of primary progressive aphasias and in prediction of progression to dementia. *Journal of Alzheimer's Disease: JAD*, *55*(1), 183–197. https://doi.org/10.3233/JAD-160682

Chen, Y., Chen, K., Zhang, J., Li, X., Shu, N., Wang, J., Zhang, Z., & Reiman, E. M. (2015). Disrupted functional and structural networks in cognitively normal elderly subjects with the APOE ε4 allele. *Neuropsychopharmacology: Official Publication of the American College of Neuropsychopharmacology*, *40*(5), 1181–1191. https://doi.org/10.1038/npp.2014.302

Chen, Y., Huang, L., Chen, K., Ding, J., Zhang, Y., Yang, Q., Lv, Y., Han, Z., & Guo, Q. (2020). White matter basis for the hub-and-spoke semantic representation: Evidence from semantic dementia. *Brain: A Journal of Neurology*, *143*(4), 1206–1219. https://doi.org/10.1093/brain/awaa057

Chen, Y., Kumfor, F., Landin-Romero, R., Irish, M., & Piguet, O. (2019). The cerebellum in frontotemporal dementia: A meta-analysis of neuroimaging studies. *Neuropsychology Review*, *29*(4), 450–464. https://doi.org/10.1007/s11065-019-09414-7

Collins, J. A., Montal, V., Hochberg, D., Quimby, M., Mandelli, M. L., Makris, N., Seeley, W. W., Gorno-Tempini, M. L., & Dickerson, B. C. (2017). Focal temporal pole atrophy and network degeneration in semantic variant primary progressive aphasia. *Brain: A Journal of Neurology*, *140*(2), 457–471. https://doi.org/10.1093/brain/aww313

Cousins, K. A. Q., Ash, S., Olm, C. A., & Grossman, M. (2018). Longitudinal changes in semantic concreteness in semantic variant primary progressive aphasia (svPPA). *Eneuro*, *5*(6), ENEURO.0197-18.2018. https://doi.org/10.1523/ENEURO.0197-18.2018

Dev, S. I., Dickerson, B. C., & Touroutoglou, A. (2021). Neuroimaging in frontotemporal lobar degeneration: Research and clinical utility. *Advances in Experimental Medicine and Biology*, *1281*, 93–112. https://doi.org/10.1007/978-3-030-51140-1_7

Ding, J., Chen, K., Liu, H., Huang, L., Chen, Y., Lv, Y., Yang, Q., Guo, Q., Han, Z., & Lambon Ralph, M. A. (2020). A unified neurocognitive model of semantics language social behaviour and face recognition in semantic dementia. *Nature Communications*, *11*(1), 2595. https://doi.org/10.1038/s41467-020-16089-9

Gorno-Tempini, M. L., Hillis, A. E., Weintraub, S., Kertesz, A., Mendez, M., Cappa, S. F., Ogar, J. M., Rohrer, J. D., Black, S., Boeve, B. F., Manes, F., Dronkers, N. F., Vandenberghe, R., Rascovsky, K., Patterson, K., Miller, B. L., Knopman, D. S., Hodges, J. R., Mesulam, M. M., & Grossman, M. (2011). Classification of primary progressive aphasia and its variants. *Neurology*, *76*(11), 1006–1014. https://doi.org/10.1212/WNL.0b013e31821103e6

Hodges, J. R., & Patterson, K. (2007). Semantic dementia: A unique clinico-pathological syndrome. *The Lancet: Neurology*, *6*(11), 1004–1014. https://doi.org/10.1016/S1474-4422(07)70266-1

Jiskoot, L. C., Panman, J. L., Meeter, L. H., Dopper, E. G. P., Donker Kaat, L., Franzen, S., van der Ende, E. L., van Minkelen, R., Rombouts, S. A. R. B., Papma, J. M., & van Swieten, J. C. (2019). Longitudinal multimodal MRI as prognostic and diagnostic biomarker in presymptomatic familial frontotemporal dementia. *Brain: A Journal of Neurology*, *142*(1), 193–208. https://doi.org/10.1093/brain/awy288

Katzman, R., Zhang, M. Y., Ouang-Ya-Qu, N., Wang, Z. Y., Liu, W. T., Yu, E., Wong, S. C., Salmon, D. P., & Grant, I. (1988). A Chinese version of the mini-mental state examination; impact of illiteracy in a Shanghai dementia survey. *Journal of Clinical Epidemiology*, *41*(10), 971–978. https://doi.org/10.1016/0895-4356(88)90034-0

Kumfor, F., Landin-Romero, R., Devenney, E., Hutchings, R., Grasso, R., Hodges, J. R., & Piguet, O. (2016). On the right side? A longitudinal study of left- versus right-lateralized semantic dementia. *Brain*, *139*(3), 986–998. https://doi.org/10.1093/brain/awv387

Lambon Ralph, M. A. (2014). Neurocognitive insights on conceptual knowledge and its breakdown. *Philosophical Transactions of the Royal Society of London. Series B, Biological Sciences*, *369*(1634), 20120392. https://doi.org/10.1098/rstb.2012.0392

Lin, Y.-H., Young, I. M., Conner, A. K., Glenn, C. A., Chakraborty, A. R., Nix, C. E., Bai, M. Y., Dhanaraj, V., Fonseka, R. D., Hormovas, J., Tanglay, O., Briggs, R. G., & Sughrue, M. E. (2020). Anatomy and white matter connections of the inferior temporal gyrus. *World Neurosurgery*, *143*, e656–e666. https://doi.org/10.1016/j.wneu.2020.08.058

Lu, J., Huang, L., Lv, Y., Peng, S., Xu, Q., Li, L., Ge, J., Zhang, H., Guan, Y., Zhao, Q., Guo, Q., Chen, K., Wu, P., Ma, Y., & Zuo, C. (2021). A disease-specific metabolic imaging marker for diagnosis and progression evaluation of semantic variant primary progressive aphasia. *European Journal of Neurology*, *28*, 2927–2939. https://doi.org/10.1111/ene.14919

Malpetti, M., Carli, G., Sala, A., Cerami, C., Marcone, A., Iannaccone, S., Magnani, G., & Perani, D. (2019). Variant-specific vulnerability in metabolic connectivity and resting-state networks in behavioural variant of frontotemporal dementia. *Cortex: A Journal Devoted to the Study of the Nervous System and Behavior*, *120*, 483–497. https://doi.org/10.1016/j.cortex.2019.07.018

Mori, S., Crain, B. J., Chacko, V. P., & van Zijl, P. C. (1999). Three-dimensional tracking of axonal projections in the brain by magnetic resonance imaging. *Annals of Neurology*, *45*(2), 265–269. https://doi.org/10.1002/1531-8249(199902)45:2<265::aid-ana21>3.0.co;2-3

Nigro, S., Filardi, M., Tafuri, B., De Blasi, R., Cedola, A., Gigli, G., & Logroscino, G. (2022). The role of graph theory in evaluating brain network alterations in frontotemporal dementia. *Frontiers in Neurology*, *13*, 910054. https://doi.org/10.3389/fneur.2022.910054

Nigro, S., Tafuri, B., Urso, D., De Blasi, R., Cedola, A., Gigli, G., Logroscino, G., & Frontotemporal Lobar Degeneration Neuroimaging Initiative. (2022). Altered structural brain networks in linguistic variants of frontotemporal dementia. *Brain Imaging and Behavior*, *16*(3), 1113–1122. https://doi.org/10.1007/s11682-021-00560-2

Patterson, K., Nestor, P. J., & Rogers, T. T. (2007). Where do you know what you know? The representation of semantic knowledge in the human brain. *Nature Reviews. Neuroscience*, *8*(12), 976–987. https://doi.org/10.1038/nrn2277

Peet, B. T., Spina, S., Mundada, N., & La Joie, R. (2021). Neuroimaging in frontotemporal dementia: Heterogeneity and relationships with underlying neuropathology. *Neurotherapeutics: The Journal of the American Society for Experimental NeuroTherapeutics*, *18*(2), 728–752. https://doi.org/10.1007/s13311-021-01101-x

Pengo, M., Premi, E., & Borroni, B. (2022). Dissecting the many faces of frontotemporal dementia: An imaging perspective. *International Journal of Molecular Sciences*, *23*(21), 12867. https://doi.org/10.3390/ijms232112867

Planche, V., Mansencal, B., Manjon, J. V., Tourdias, T., Catheline, G., Coupé, P., & Frontotemporal Lobar Degeneration Neuroimaging Initiative and the National Alzheimer's Coordinating Center cohort. (2023). Anatomical MRI staging of frontotemporal dementia variants. *Alzheimer's & Dementia: The Journal of the Alzheimer's Association*. Published online 07 February 2023. https://doi.org/10.1002/alz.12975

Playfoot, D., Billington, J., & Tree, J. J. (2018). Reading and visual word recognition ability in semantic dementia is not predicted by semantic performance. *Neuropsychologia*, *111*, 292–306. https://doi.org/10.1016/j.neuropsychologia.2018.02.011

Reber, T. P., Bausch, M., Mackay, S., Boström, J., Elger, C. E., & Mormann, F. (2019). Representation of abstract semantic knowledge in populations of human single neurons in the medial temporal lobe. *PLoS Biology*, *17*(6), e3000290. https://doi.org/10.1371/journal.pbio.3000290

Reyes, P., Ortega-Merchan, M. P., Rueda, A., Uriza, F., Santamaria-García, H., Rojas-Serrano, N., Rodriguez-Santos, J., Velasco-Leon, M. C., Rodriguez-Parra, J. D., Mora-Diaz, D. E., & Matallana, D. (2018). Functional connectivity changes in behavioral, semantic, and nonfluent variants of frontotemporal dementia. *Behavioural Neurology*, *2018*, 9684129. https://doi.org/10.1155/2018/9684129

Rubinov, M., & Sporns, O. (2010). Complex network measures of brain connectivity: Uses and interpretations. *NeuroImage*, *52*(3), 1059–1069. https://doi.org/10.1016/j.neuroimage.2009.10.003

Schwab, S., Afyouni, S., Chen, Y., Han, Z., Guo, Q., Dierks, T., Wahlund, L.-O., & Grieder, M. (2020). Functional connectivity alterations of the temporal lobe and hippocampus in semantic dementia and Alzheimer's disease. *Journal of Alzheimer's Disease: JAD*, *76*(4), 1461–1475. https://doi.org/10.3233/JAD-191113

Simmons, W. K., Ramjee, V., Beauchamp, M. S., McRae, K., Martin, A., & Barsalou, L. W. (2007). A common neural substrate for perceiving and

knowing about color. *Neuropsychologia*, *45*(12), 2802–2810. https://doi.org/10.1016/j.neuropsychologia.2007.05.002

Staffaroni, A. M., Ljubenkov, P. A., Kornak, J., Cobigo, Y., Datta, S., Marx, G., Walters, S. M., Chiang, K., Olney, N., Elahi, F. M., Knopman, D. S., Dickerson, B. C., Boeve, B. F., Gorno-Tempini, M. L., Spina, S., Grinberg, L. T., Seeley, W. W., Miller, B. L., Kramer, J. H., … Rosen, H. J. (2019). Longitudinal multimodal imaging and clinical endpoints for frontotemporal dementia clinical trials. *Brain*, *142*(2), 443–459. https://doi.org/10.1093/brain/awy319

Sundqvist, M., Routier, A., Dubois, B., Colliot, O., & Teichmann, M. (2020). The white matter module-hub network of semantics revealed by semantic dementia. *Journal of Cognitive Neuroscience*, *32*(7), 1330–1347. https://doi.org/10.1162/jocn_a_01549

Tao, Y., Ficek, B., Rapp, B., & Tsapkini, K. (2020). Different patterns of functional network reorganization across the variants of primary progressive aphasia: A graph-theoretic analysis. *Neurobiology of Aging*, *96*, 184–196. https://doi.org/10.1016/j.neurobiolaging.2020.09.007

Tulving, E. (1972). Episodic and semantic memory. In E. Tulving & W. Donaldson (Eds.), *Organization of memory* (pp. 381–403). Academic Press.

Tzourio-Mazoyer, N., Landeau, B., Papathanassiou, D., Crivello, F., Etard, O., Delcroix, N., Mazoyer, B., & Joliot, M. (2002). Automated anatomical labeling of activations in SPM using a macroscopic anatomical parcellation of the MNI MRI single-subject brain. *NeuroImage*, *15*(1), 273–289. https://doi.org/10.1006/nimg.2001.0978

Vignando, M., Rumiati, R. I., Manganotti, P., Cattaruzza, T., & Aiello, M. (2020). Establishing links between abnormal eating behaviours and semantic deficits in dementia. *Journal of Neuropsychology*, *14*(3), 431–448. https://doi.org/10.1111/jnp.12195

Wagner, A. D., Paré-Blagoev, E. J., Clark, J., & Poldrack, R. A. (2001). Recovering meaning: Left prefrontal cortex guides controlled semantic retrieval. *Neuron*, *31*(2), 329–338. https://doi.org/10.1016/s0896-6273(01)00359-2

Wang, J., Wang, X., Xia, M., Liao, X., Evans, A., & He, Y. (2015). GRETNA: A graph theoretical network analysis toolbox for imaging connectomics. *Frontiers in Human Neuroscience*, *9*, 386. https://doi.org/10.3389/fnhum.2015.00386

Wang, J.-H., Zuo, X.-N., Gohel, S., Milham, M. P., Biswal, B. B., & He, Y. (2011). Graph theoretical analysis of functional brain networks: Test-retest evaluation on short- and long-term resting-state functional MRI data. *PLoS One*, *6*(7), e21976. https://doi.org/10.1371/journal.pone.0021976

Woollams, A. M., & Patterson, K. (2018). Cognitive consequences of the left-right asymmetry of atrophy in semantic dementia. *Cortex: A Journal Devoted to the Study of the Nervous System and Behavior*, *107*, 64–77. https://doi.org/10.1016/j.cortex.2017.11.014

Younes, K., Borghesani, V., Montembeault, M., Spina, S., Mandelli, M. L., Welch, A. E., Weis, E., Callahan, P., Elahi, F. M., Hua, A. Y., Perry, D. C., Karydas, A., Geschwind, D., Huang, E., Grinberg, L. T., Kramer, J. H., Boxer, A. L., Rabinovici, G. D., Rosen, H. J., … Gorno-Tempini, M. L. (2022). Right temporal degeneration and socioemotional semantics: Semantic behavioural variant frontotemporal dementia. *Brain: A Journal of Neurology*, *145*(11), 4080–4096. https://doi.org/10.1093/brain/awac217

Younes, K., & Miller, B. L. (2020). Frontotemporal dementia: Neuropathology, genetics, neuroimaging, and treatments. *The Psychiatric Clinics of North America*, *43*(2), 331–344. https://doi.org/10.1016/j.psc.2020.02.006

Yu, Q., Mai, Y., Ruan, Y., Luo, Y., Zhao, L., Fang, W., Cao, Z., Li, Y., Liao, W., Xiao, S., Mok, V. C. T., Shi, L., Liu, J., & National Alzheimer's Coordinating Center, the Alzheimer's Disease Neuroimaging Initiative, & Frontotemporal Lobar Degeneration Neuroimaging Initiative. (2021). An MRI-based strategy for differentiation of frontotemporal dementia and Alzheimer's disease. *Alzheimer's Research & Therapy*, *13*(1), 23. https://doi.org/10.1186/s13195-020-00757-5

SUPPORTING INFORMATION

Additional supporting information can be found online in the Supporting Information section at the end of this article.

How to cite this article: Huang, L., Cui, L., Chen, K., Han, Z., & Guo, Q. (2023). Functional and structural network changes related with cognition in semantic dementia longitudinally. *Human Brain Mapping*, 1–12. https://doi.org/10.1002/hbm.26345